Energy Technology
Generation, Conversion, Storage, Distribution
www.entechnol.de

Flexible Bielectrode-Based Highly Sensitive Triboelectric Motion Sensor: A Sustainable and Smart Electronic Material

*Damian Zamora, Abu Musa Abdullah, Alejandro Flores, Haimanti Majumder, Muhtasim Ul Karim Sadaf, Bahareh Azimi, Serena Danti, and M. Jasim Uddin**

The self-powered and autonomous sensors are incredibly important in advanced engineering, especially defence science. The increasing necessity of simple and smart electronics requires to be sustainably flexible, wearable, and waterproof. Triboelectricity has been a widely used mechanism for motion sensing nowadays. Almost all devices based on triboelectricity require contact between two surfaces. Herein, a touchless triboelectric motion sensor for human motion sensing and movement monitoring is developed. The device was primarily fabricated using simple latex (cis-1,4-polyisoprene) structures and copper (electrode materials), which make it a very cost-effective device for sensory applications. The device is tested with specimens of different areas and heights in motion. The maximum output of the device is noted as 12 V at a specimen height of 5 cm. Further different types of human motions are applied in front of the device to ensure low energy sensitivity using triboelectric phenomena. The lightweight smart device precisely provides significant output signals for each movement of the human body which makes the device a prospective medium for motion sensing and movement monitoring which can be applied in the fields of security, energy, and medicine.

1. Introduction

Triboelectric and piezoelectric technologies have made great strides in the research community since 2012.[1–3] With an enlightened perspective on the future applications, these methods have been sought out by researchers to determine different practical applications. Triboelectricity is a rapidly expanding form of science that is constantly being changed and there is still much to be tested to determine the most optimal combination of material and their possible functions.[4–7] In the past, motion sensors have been limited to a finite number of concepts all of which are either highly priced or inaccurate. Methods such as a thermal recognition sensor and imaging optics are the most widely used in today's motion sensors.

Thermal sensors are primarily designed with the technology to detect a change in temperature caused by a foreign object entering a room and emitting a relatively significant amount of a thermal signature.[8] The thermal sensors are prone to be in triggered by the heat signatures from animals, thus limiting the device to indoor or other secluded areas. The imaging optics, in contrast, are constantly capturing images and are designed to detect when an image taken has an anomaly from the images prior.[9] This event leaves for a highly sensitive motion detector that is constantly being triggered by inanimate objects and animals making it insufficient for a variety of environments. Another more common type of motion sensor uses wave technology such as the sound wave from an ultrasonic frequency that detects a shift as the sound echoes back to the device.[9–12] This type of sensor can be paired with the technology of thermal or imaging sensors to create a more accurate sensor, but the price of the quality product can be upwards of 100 USD only for one device. Another kind of sensor, commonly known as IR passive sensor, emits IR radiation toward a target area, then reflectance is measured continuously with a light sensor.[13] Whenever a change in target area occurs, the reflectance triggers the sensor, and the system detects motion. This kind of sensor is very common in everyday life. Present-day security systems largely depend on it.[14] Due to the limitation in using IR passive sensors in the heated area or with other light sources, their practical applications in diverse fields have been faced with limitations.

Triboelectricity has been widely used for diverse engineering applications like mechanical energy harvesting and sensing applications.[15–18] Particularly, triboelectric nanogenerator has been an emerging technology for motion sensing and pressure sensing applications.[3,7,19] This research focuses on a

D. Zamora, A. M. Abdullah, A. Flores, H. Majumder, M. U. K. Sadaf, M. J. Uddin
Department of Chemistry
Photonics and Energy Research Laboratory-PERL
University of Texas Rio Grande Valley
Edinburg, TX 78539, USA
E-mail: mohammed.uddin@utrgv.edu

A. M. Abdullah, A. Flores
Department of Mechanical Engineering
University of Texas Rio Grande Valley
Edinburg, TX 78539, USA

B. Azimi, S. Danti
Department of Civil and Industrial Engineering
Università di Pisa
56126 Pisa PI, Italy

The ORCID identification number(s) for the author(s) of this article can be found under https://doi.org/10.1002/ente.202100662.

DOI: 10.1002/ente.202100662

triboelectricity-based device that is able to create an identical output signal with motion which is determined by the size and distance of the foreign object with respect to the device. Unlike any other fabricated motion sensors, the triboelectric motion sensor (TEMS) uses triboelectricity to perform its operation and it can be used as a sensor and detector without any external power source. That gives TEMS a huge advantage because all modern-day sensors or detectors mostly rely on some sort of external power source. This cost-effective and simple structured unique device is designed for the accurate detection of different motions at a certain range without the touch between two solid surfaces. Besides, the intensity of signals has been tested for variable distances from a certain object. Copper metal and latex are primarily used as triboelectric materials for the device. Due to the low cost and availability of the materials, the device is suitable for mass production as a technology for tracking and security purposes. Even if the range on the device is limited, the low cost for the product will allow for it to be bought in bulk so it can be placed throughout a location and ensure that a constant blanket of motion detection is maintained. The TEMS has the potential to be adjusted for multiple uses from sensors, to an energy source, or even used in the currently expensive medical technology to reduce costs.[20–22]

2. Results and Discussion

Figure 1a,b depicts a view of TEMS and the individual material in an expanded and collapsed view. The test setup of the TEMS with markings for different heights is shown in Figure 1c. The internal components are also represented by Figure 1d with a cut in the completely assembled TEMS. The green layer with an inner grey tube represents the latex (polychloroprene) sample from a commercial balloon enclosing a hollow steel ring and has been placed so that the latex is relatively covering the bottom opening of the ring. This latex layer was then laid on top of a blank copy paper that is depicted by the red ring. Then it was followed by the circular copper sheet, represented by the yellow layer, which is located on the bottom of the TEMS and would be used as an electrode for the device.

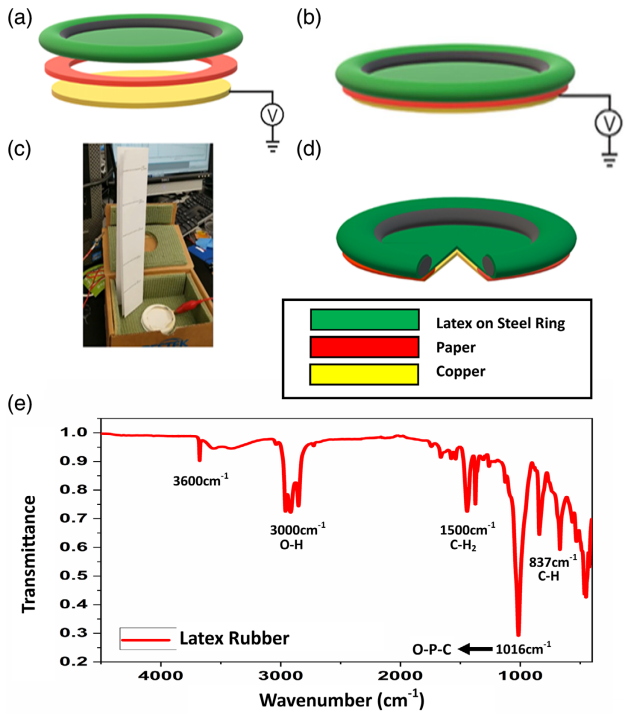

Figure 1. Schematic view of triboelectric motion sensor: a) disassembled and b) assembled. c) TEMS test setup. d) Cut-out of the assembled TEMS. e) Fourier transform infrared ray (FTIR) of polychloroprene/latex.

Fourier transform infrared ray (FTIR) spectrum of nitrile rubber is demonstrated in Figure 1e. The peak at 837 cm^{-1} demonstrates a strong C–H out of plane bending.[23,24] The characteristic band at 1016 cm^{-1} attributed to O–P–) asymmetric stretching caused by phospholipids. It can be further clarified as stretching of O–P–C.[25] The multiple peaks around 1500 cm^{-1} are associated with CH_2 deformations. A broader peak at 3000 cm^{-1} demonstrates the presence of hydroxyl group along with nitrile latex. This is also associated with C—H bonding deformation in the same region. A blue shift is present in these peaks. Stretching of C–H and O–H is responsible for the peak in 3600 cm^{-1}. This demonstrates the integrity of commercially available rubber as laboratory-grade rubber. It also demonstrates the absence of any other interfering materials in our experiment.

The latex was favorable for its elasticity as it remained in a constant stretched position throughout the testing with no complications.[26] The only drawback was that the TEMS was constructed ensuring that the latex was evenly stretched across the surface area to prevent inconsistent results. The steel ring, as a foundation around which the rest of the TEMS would be designed, provided the stability. The circular structure was beneficial in achieving a 360° sensor, but the conductivity of the steel was a factor that resulted in the need for a buffer from the copper sheet. Since an unbuffered design failed to produce any reliable results; later, an insulator buffer was added. Standard copy paper was used as it was easily cut to design, and the thin dimension allowed for accurate and minuscule buffer heights to be adjusted for testing.

Figure 2a,b illustrates the working mechanism of the TEMS in motion and no motion condition, respectively. The layer of cellulose paper acts as a nonconducting spacer to provide a degree of latex movement and to prevent an interrupted flow of electrons between the latex and copper. The copper can act as an electrode to transfer free-floating electrons and create a voltage that can then be measured or harnessed in the form of potential energy.[27] The latex is a negative triboelectric material that holds negatively charged electrons more profoundly to the surface toward copper.[28,29] The movement of the body near the device leads to the air pressure changes above the latex layer. Latex is introduced to the frictional nitrogen and oxygen from the air floating above it. Stretched latex rubber is very much susceptible to the friction caused by the floating nitrogen and oxygen molecules.[30] Through the movement of an object surrounding the TEMS and air displacement, the nitrogen and oxygen molecules in the atmosphere can create this environment of friction.[31] The latex layer gets charged due to the stretch of the latex as a result of the friction with air.[32] Simultaneously, as the latex is creating static electricity from the friction of the molecules, an electron transfer is conducted as the latex vibrates from the change in

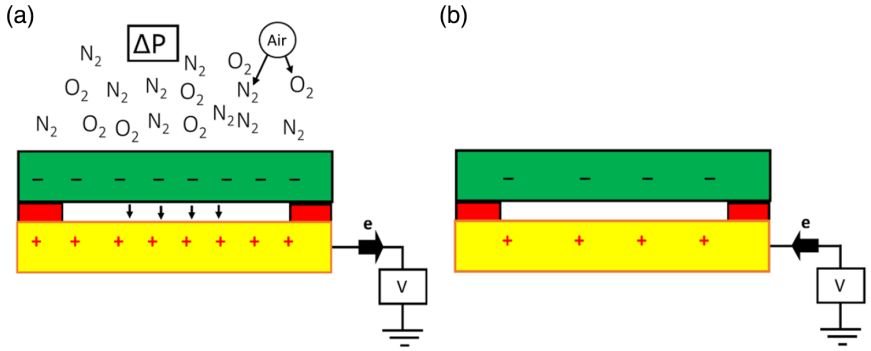

Figure 2. Mechanism of triboelectric motion sensor in: a) motion stage, b) no motion stage.

air pressure thus reducing the distance to the copper electrode at a very small precision. The latex accumulates electrons and gets negatively charged at this stage. With the shortened distance and negative charge of the latex, the electricity field surrounding the latex will affect the copper electrode which will result in triboelectrification and electrostatic induction.[3,10] Electrons will flow toward the ground from the copper electrode to neutralize this effect of triboelectrification and electrostatic induction (Figure 2a).[33] The copper ions which hold a positive charge create a path for the electrons to travel throughout the electrode where they can be measured and utilized.[34] Throughout the entirety of this process, the copper molecules will lose electrons to become copper ions. This will in turn create free-floating electrons which will also flow out through the electrode.[35] As motion is withdrawn near the sensor, the air pressure also gets back to its initial stage. The latex rubber loses its negative charges and the whole process gets reversed. The electron flows to the electrode from the ground to neutralize the positive ions of the copper electrode at this stage (Figure 2b).[33,36] The negative voltage will be generated eventually providing an AC signal from the device. The amplitude of the output signal is not expected to be high since the friction in the latex layer occurs on a low scale.

The results suggest that it is the displacement of gas molecules in the environment, such as N_2 and O_2, that produce a static electricity charge by the means of friction along the latex surface of the TEMS.[37] The sheet of copper is an electron-rich material and is known to have free-floating electrons within the molecules which can be harnessed by the means of electron transfers. The electron-rich air of the atmosphere is primarily composed of nitrogen and oxygen molecules and they conduct an electron transfer with the latex as it is displaced by movement, producing an electron-rich environment on the top portion of the TEMS. The now electron-rich latex creates an electric field that repulses the electrons found in copper and attracts the protons to the area of copper closest to the latex. The free-floating electrons found in copper are then repelled from the electrode of the TEMS and can be harnessed to generate and measure the potential energy.

Figure 3 depicts the results of specimens with various surface areas tested above the TEMS with different heights. For this category of testing, aluminum sheets were cut into squares of 5 cm by 5 cm and increased by increments of 5 cm until they became 20 cm by 20 cm. To conduct the testing, the sheets were held by clamps and moved over the TEMS, traveling from right to left. After each successful pass, the aluminum layer was placed below the device and the process was repeated with the subsequent sample until all samples completed a smooth consistent movement.

At the height of 10 cm and 25 cm, a trend of a higher voltage was observed by increasing the surface area of the specimen. The heights of 35 and 40 cm were so excessive that increasing the size of the surface area being tested did not distinctly generate the same trend of data as the previous heights but instead clearly showed prolonging peaks as the surface area increased. The increased height made for a larger number of molecules in the atmosphere to be displaced, but at a slower rate which explains the lower voltage at an extended duration. The maximum output voltage was observed to be 1.3 V for $20 \times 20\,cm^2$ surface area of the Al sheet at 10 cm height. It is also important to note that as the height increased from the TEMS, the overall voltage being detected reduced. There was a distinct change in voltage values when transitioning between 10 and 25 cm but relatively minimal differences from 35 to 40 cm. The air pressure is more distributed at a higher distance. Therefore, the TEMS is more sensitive to the motions at the lower heights.

The effect of adjusting the gap of the buffer that separates the latex and copper materials from each other was very drastic on the amount of potential energy detected (**Figure 4**). The trend of the data was consistent, in that it continuously decreased as the distance from the TEMS increased. The distance of 40 cm demonstrated the lowest voltage in comparison to the other distances. It was also observed that the peaks would plateau at relatively low voltages with the increment of buffer distance. So, while the trend remained consistent, a quite noticeable change in the output of potential energy continued to diminish as the buffer distance increased.

After repeated testing at several distances, the 0.2 mm gap achieved the desired results of over 12 V at the nearest height, as well as a distinct detection (peak) at 40 cm, without increasing the sensitivity of the TEMS device itself. It can be deemed that at closer buffer distances, the device would become very sensitive to the surrounding environment that it would record the data which is detected from an individual just standing near the device. Again, the theory of the movement of the electrons becomes evident due to a constant decline of potential energy when movement is not conducted by the device and it results in a consistent loss of the free-floating electrons through the

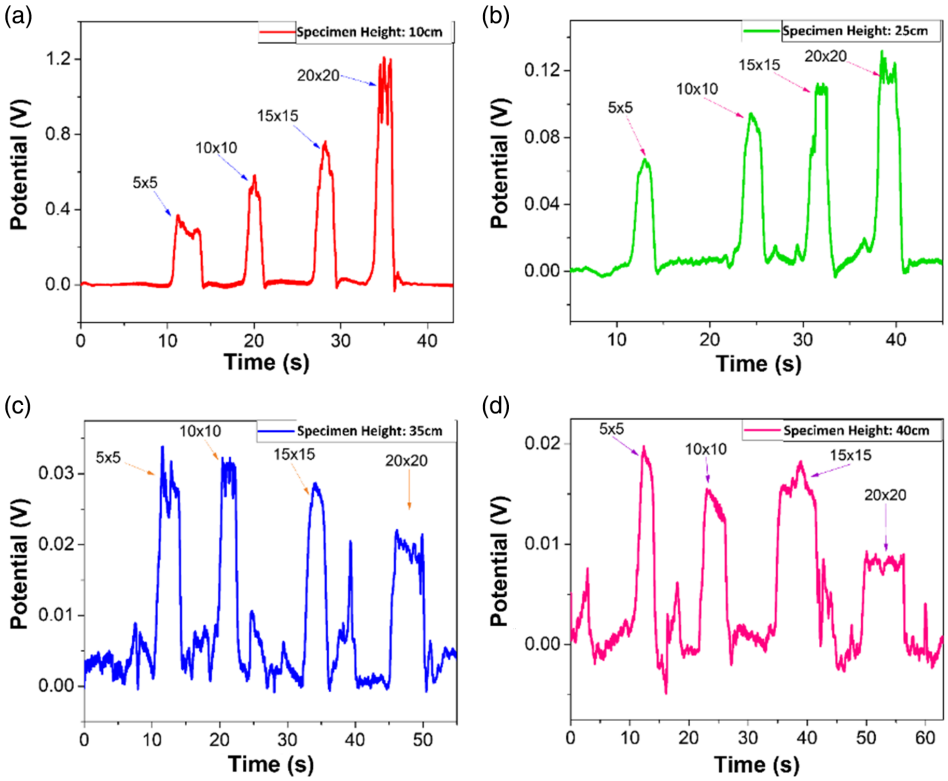

Figure 3. Test of different sized specimens (shown in the figures as length(cm) × width(cm)) from heights of: a) 10 cm, b) 25 cm, c) 35 cm, and d) 40 cm.

electrode. Regardless of the number of electrons that have flowed through the electrode of TEMS, when the TEMS detects a specific movement, the resulting recorded voltage has the same specific value every time the same movement is conducted. For example, the TEMS at rest is at a constant decline and after 5 s has elapsed, an event such as a finger snap will result in roughly 0.1 V. Whereas, after 1 min (or any length of time), the results will still be roughly 0.1 V for the same movement.

The data gathered from multiple types of body motions further supports the evidence of the amount of displacement of the molecules in the air. These are the determining factors of the amount of potential energy from the TEMS which can be observed in the graphs as signal intensity v/v_o, in which v_o being the maximum value observed. The finger-snapping movement shown in **Figure 5**a,d, was the most consistent movement. The different ranges of peaks can be determined by the exaggeration of the individual fingers. It was also determined that only gesture of finger-snapping affected the device, not noise. A snap without noise generated similar results to the noise-producing counterparts. These phenomena could have been produced due to the sensibility of the TEMS identifying the potential energy passively produced in the laboratory where it has been tested. The subjects that produce these counterparts were identified as any machine, tool, or any other subject that could create a vibration creating potential energy consequently.

Figure 5b,c reflect the data when a person is walking with an emphasis on the movement of the lower body extremities, so the arm swing had a minimal effect. It was first tested by comparing 5 consecutive raising and lowering of the left leg followed by the right leg while the rest of the body remained stationary. The minute differences in the locations of the legs affected the data drastically, from the height of each repetition to the distance from the TEMS, each of which varied by no more than 2 inches between the left and right leg. This event was also supported by the following tests as the test subject remained stationary but instead alternated the raising and lowering of each leg. This test showed a more consistent correlation between the peaks of the corresponding leg raises, which would again show a relatively small range of the peaks of data. The smoother graphical response in Figure 5e,f demonstrates the stationary movement of the human body.

The TEMS was also tested by walking forward and backward from the device with the purpose of identifying the sensitivity of the device with the movement of an object. **Figure 6**a shows a representation of the previous statement. Figure 6b,c represents data gathered from the same test subject from the previous figures who walked toward and away from the TEMS at a controlled distance and pace. Figure 6b was performed with the subject walking back and forth from the device, this is approaching and distancing from it. The motion created by the human body is identified as signal intensity v/v_o, v_o is the maximum value observed, creating peak-to-peak values. The lower peaks in the graph mean that the subject was distancing from the device, and higher peaks mean the data gathered when the subject was approaching it. It was observed that when the subject was moving backward from the TEMS the peaks had a maximum signal intensity of 0.6, and when moving forward to the device the highest peaks were above 0.86. Figure 6c represents the data taken when the subject was moving forward and

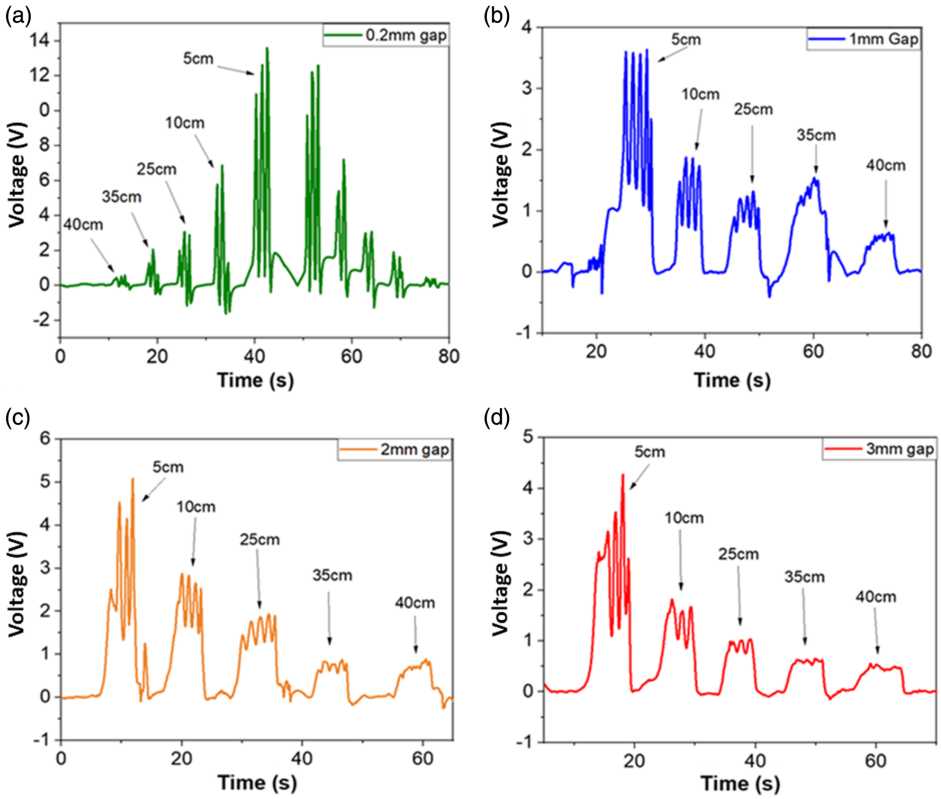

Figure 4. Test of the specimen from the same height with differing distances between the triboelectric layers of: a) 0.2 mm, b) 1 mm, c) 2 mm, and d) 3 mm.

backward from the device, this was tested by walking next to it. The data was identified as signal intensity v/v_o, v_o being the maximum value observed. The higher peaks were around 0.8, and the lower peaks were around 0.8 as well. The graph in Figure 6c has larger gaps between peaks due to the speed of the subject when testing because it was done at a slower pace. Figure 6d,e represents the extended view of the output. When moving closer to the device, the potential energy increased appropriately and would drop to nearly 0 immediately and return to the peak as the test subject began moving away from the device. As the test subject would stop at the furthest distance from the device, the data would then plateau at a higher value than when stopping at a close distance. This event would be explained by the slight, but constant movement of the individual's body as the test subject changes direction and the device continues to remain in a charged state from the previous movement. Overall, this figure supports the fact that the speed at which an object travels does not affect the potential energy significantly, but it is the distance and size of the test subject that contribute to the attained data. The recorded data from the movement of a single hand was significantly smaller than the data from that of a whole limb or an individual. Since the data from the leg movement was similar to that of an entire human body, it can be stated that there is a maximum value of potential energy that can be reached based on mass alone. This type of output response can be utilized to measure stepping or walking speed.

Overall, the consistent output produced by the TEMS may be impactful in many practical applications as well as a base of concept for other concepts. The highly sensitive nature of the device which utilizes the movement of molecules in the environment can be employed in areas with high volumes of traffic with the prospects detecting the amount of movement nearby while maintaining a constant flow of energy that could be harnessed to provide power.

3. Experimental Details

3.1. Device Fabrication

The different materials utilized were a sheet of copper, steel ring, latex balloon, copy paper, and gorilla glue. The materials were shaped into a circle of 1.5 inch diameter with the sheet of copper as the bottommost layer. The second layer consisted of 2 stacked sheets of paper, which were cut into a ring to not affect the electric field throughout the system. The final layer was made up of a steel ring with an outstretched latex balloon attached by the means of gorilla glue on the sides of the ring. Extra caution was taken to ensure that the latex was stretched evenly throughout the ring as it was being attached. The copper was laid on the surface with the sheets of paper, acting as a buffer, carefully placed on top. The steel ring with the latex on the bottom was then placed on top of the sheets of paper, ensuring that none

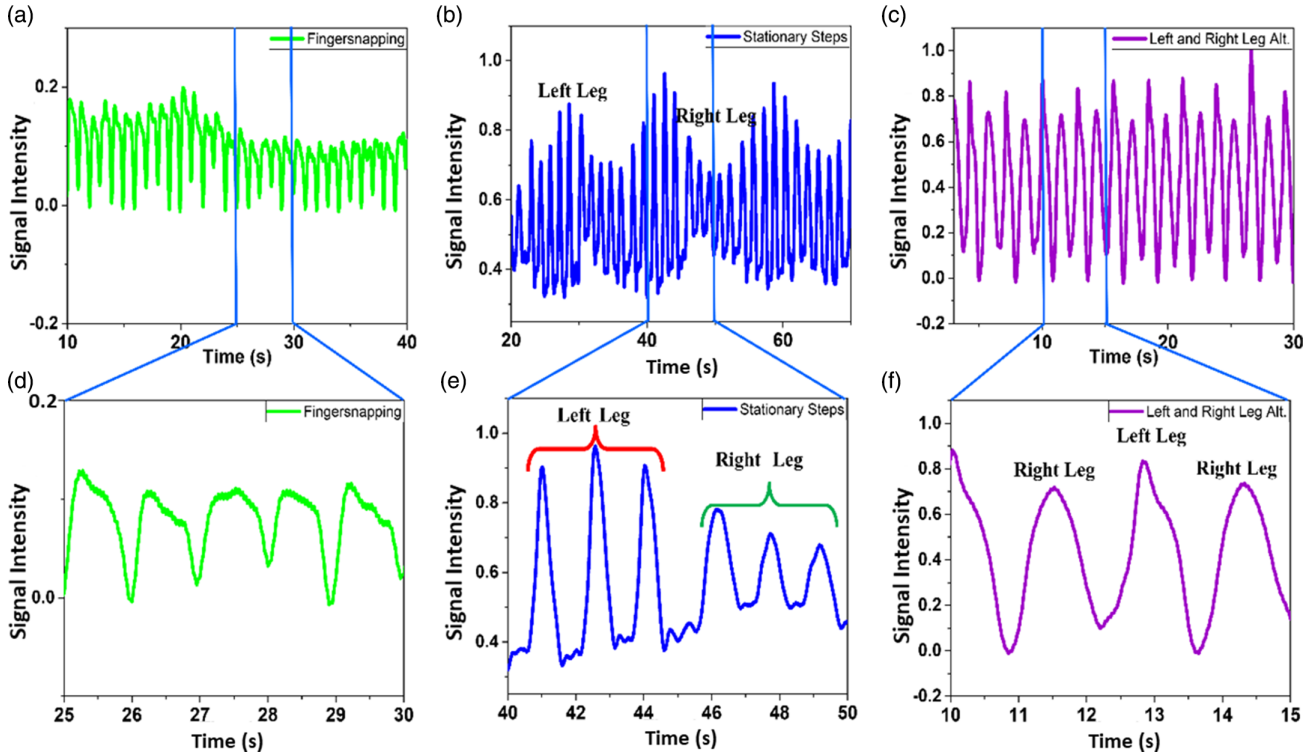

Figure 5. Response intensity of the motion sensor on: a) finger-snapping, b) stationary leg movement, c) alternating leg movement, d) enlarged view on finger-snapping, e) enlarged view on stationary leg movement, and f) enlarged view on alternating leg movement.

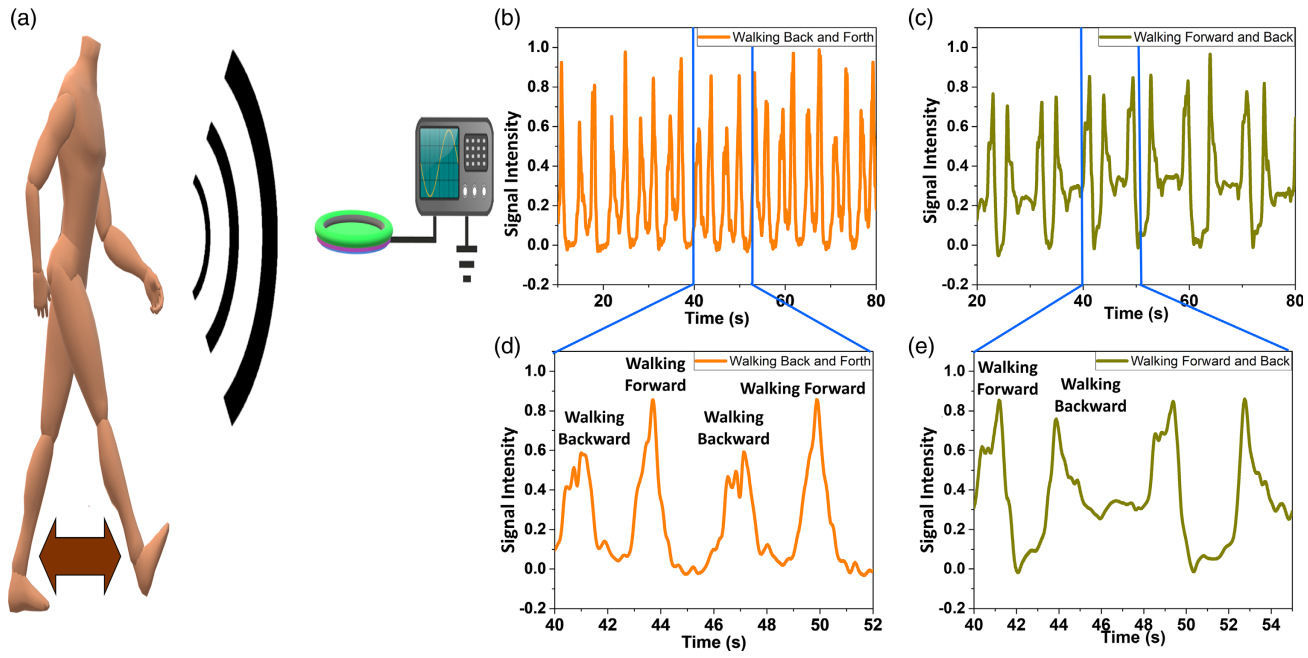

Figure 6. a) Schematic view of the walking test with TEMS. The output response of the TEMS on: b) walking back and forth, c) walking forward and backward. Enlarged view of the output response for: d) walking backward and forward and e) walking forward and backward.

of the materials shifted during this process so that there was a small gap between the latex and copper. The assembled device was then placed into a small cardboard box that was lined internally with a 0.5 inch thick sheet of foam.

3.2. Frequency-Absorbing Chamber Fabrication

The purpose of the frequency-absorbing chamber was to isolate the device from the external environment to reduce any anomalies during testing. During initial testing without the chamber, the TEMS was found to be extremely sensitive to the environment and proved to be inconsistent. The chamber was constructed with a cellulose-made box from a commercial supplier with polystyrene foam attached to the whole surface. Testing was conducted with the TEMS placed on top of a table that was fixed with the floor which ensured minimum noise, but the device would begin to charge and discharge a varied amount of energy constantly. This event would become more apparent when the TEMS would detect movement as soon as an individual began raising their arm holding the sample. Due to this, it could not be determined whether data was being generated due to the sample alone or due to the movement of the body, expressing the necessity of isolating the device from external inconsistencies.

3.3. Output Signal Characterization

The TEMS was connected to the VersaSTAT3 with a single connection to the TEMS itself, and a ground attached to the cardboard box. Open-circuit voltammetry was applied for the experiment. The top of the box was kept open to the channel during the movement being tested. As different forms of the movement were tested and the data were compared, it became clear that not only did direction and speed affect the results, but the size of the person conducting the movement also played an influential role. This event was tested by having 3 research members walk past the TEMS in sequential order from shortest to tallest, and the results correlated with the individual's size. Essentially, with more mass that was conducting a movement, the TEMS recorded with higher potential energy output and vice versa with a lower mass.

3.4. FTIR Characterization

Perkin Elmer Lambda IR Spectrometer was used for the Fourier Transform Infrared spectroscopy of the NBR rubber. The transmittance of the NBR was measured from 400 to 4500 cm^{-1}. The test was performed at a resolution of 4 cm^{-1}.

4. Conclusion

In conclusion, a touchless motion sensor was developed based on latex and copper for motion sensing and movement monitoring. The resulting output signals at variable movements have been highly consistent. Distance of the subject from the TEMS proved to be the crucial determining factor as the intensity of the output signal varied with distances of mere centimetres. The surface area also played a major role in the results as a small surface area showed a quick and relatively high voltage. Whereas the larger surface area showed a prolonged but relatively lower amount of voltage. This new method of utilizing a highly sensitive triboelectric device by means of a motion sensor has many more possible applications that have yet to be determined. There are many different methods of utilization for a motion detector that costs no more than $5 to produce and are created by items found in a local hardware store. The practical applications other than as a motion sensor are endless with the combination of materials that are easily replaceable and interchangeable. This unique concept derived from triboelectric technology has the potential for different sensory applications other than detecting motion, it may even be manipulated to be utilized as a small-scale energy source such as home lighting as people walk throughout the building. The TEMS is surely a device that when connected with multiple units, will prove to be invaluable in the fields of security, energy, and possibly even as a monitor to track the human body for medical and athletic purposes.

Acknowledgements

This research was supported by National Science Foundation (NSF PREM) Award # 2122178 UTRGV-UMN Partnership to strengthen the PREM pathway. This project was partially supported by the Welch Foundation Award # BX-0048-20211024 and Elliot the Elliott Chemical Society. The authors thank Aminur Rashid Choudhury for fruitful discussion and support.

Conflict of Interest

The authors declare no conflict of interest.

Data Availability Statement

The data that support the findings of this study are available from the corresponding author upon reasonable request.

Keywords

motion sensing, potential energy sensing, sustainable triboelectric sensor, triboelectricity

Received: July 31, 2021
Revised: November 3, 2021
Published online: February 3, 2022

[1] Z. L. Wang, J. Song, *Science* **2006**, *312*, 242.
[2] F.-R. Fan, Z.-Q. Tian, Z. Lin Wang, *Nano Energy* **2012**, *1*, 328.
[3] A. R. Chowdhury, A. M. Abdullah, I. Hussain, J. Lopez, D. Cantu, S. K. Gupta, Y. Mao, S. Danti, M. J. Uddin, *Nano Energy* **2019**, *61*, 327.
[4] B.-Y. Lee, D. H. Kim, J. Park, K.-I. Park, K. J. Lee, C. K. Jeong, *Sci. Technol. Adv. Mater.* **2019**, *20*, 758.
[5] S. S. Indira, C. A. Vaithilingam, K. S. P. Oruganti, F. Mohd, S. Rahman, *Nanomaterials* **2019**, *9*, 773.
[6] A. R. Chowdhury, J. Jaksik, I. Hussain, P. Tran, S. Danti, M. J. Uddin, *Energy Technol.* **2019**, *7*, 1800767.
[7] A. M. Abdullah, A. R. Chowdhury, Y. Yang, H. Vasquez, H. J. Moore, J. G. Parsons, K. Lozano, J. J. Gutierrez, K. S. Martirosyan, M. J. Uddin, *J. Mol. Liq.* **2020**, *297*, 111982.
[8] D. J. Welbourne, A. W. Claridge, D. J. Paull, A. Lambert, *Remote Sens. Ecol. Conserv.* **2016**, *2*, 77.
[9] C. Y. Yong, R. Sudirman, K. M. Chew, in *Modelling Simulation 2011 Third Inter. Conf. on Computational Intelligence*, Langkawi, Malaysia **2011**, pp. 46–50.
[10] Y. Tang, H. Zhou, X. Sun, N. Diao, J. Wang, B. Zhang, C. Qin, E. Liang, Y. Mao, *Adv. Funct. Mater.* **2020**, *30*, 1907893.

[11] A. M. Zungeru, *Int. J. Secur. Privacy Trust Manage.* **2013**, *2*, 1.
[12] A. P. Arguelles, J. A. Turner, *J. Acoust. Soc. Am.* **2017**, *141*, 4347.
[13] K. Ota, Y. Ota, M. Otsu, A. Kajiwara, *2011 IEEE Sensors Applications Symp.*, IEEE, Piscataway, NJ **2011**, https://doi.org/10.1109/SAS.2011.5739786.
[14] M. Ostrovsky, P. Soccoli, W. Rose, A. Lombardi, J. Porter, US20060125624A1, **2006**, https://patents.google.com/patent/US20060125624A1/en (accessed: March 2020).
[15] M. Ma, Z. Kang, Q. Liao, Q. Zhang, F. Gao, X. Zhao, Z. Zhang, Y. Zhang, *Nano Res.* **2018**, *11*, 2951.
[16] A. M. Abdullah, A. Flores, A. R. Chowdhury, J. Li, Y. Mao, M. J. Uddin, *Nano Energy*, **2020**, *73*, 104774.
[17] D. Lopez, A. R. Chowdhury, A. M. Abdullah, M. U. K. Sadaf, I. Martinez, B. D. Choudhury, S. Danti, C. J. Ellison, K. Lozano, M. J. Uddin, *Energy Technol.* **2021**, *9*, 2001088.
[18] A. M. Abdullah, M. U. K. Sadaf, F. Tasnim, H. Vasquez, K. Lozano, M. J. Uddin, *Nano Energy* **2021**, *86*, 106133.
[19] A. R. Chowdhury, A. M. Abdullah, U. V. Romero, I. Hussain, C. Olivares, S. Danti, J. Li, M. J. Uddin, *Med. Devices Sens.* **2020**, *3*, 10103.
[20] C. Wu, A. C. Wang, W. Ding, H. Guo, Z. L. Wang, *Adv. Mater.* **2019**, *9*, 1802906.
[21] H.-J. Yoon, H. Ryu, S.-W. Kim, *Nano Energy* **2018**, *51*, 270.
[22] Q. Zheng, B. Shi, Z. Li, Z. L. Wang, *Adv. Sci.* **2017**, *4*, 1700029.
[23] A. Linos, M. M. Berekaa, R. Reichelt, U. Keller, J. Schmitt, H.-C. Flemming, R. M. Kroppenstedt, A. Steinbüchel, *Appl. Environ. Microbiol.* **2000**, *66*, 1639.
[24] D. Kowalczuk, M. Pitucha, *Materials* **2019**, *12*, 2972.
[25] J. M. Nzai, A. Proctor, *J. Am. Oil Chem Soc.* **1998**, *75*, 1281.
[26] W. A. Osborne, W. Sutherland, *Proc. R. Soc. London Ser. B* **1909**, *81*, 485.
[27] R. H. Fowler, *Proc. R. Soc. London Ser. A* **1933**, *141*, 56.
[28] P. Egberts, R. W. Carpick, Viewpoint: Friction at the Atomic Scale, Physics, 6, **2013**, https://physics.aps.org/articles/v6/102 (accessed: March 2020).
[29] A. E. Wang, P. S. Gil, M. Holonga, Z. Yavuz, H. T. Baytekin, R. M. Sankaran, D. J. Lacks, *Phys. Rev. Mater.* **2017**, *1*, 035605.
[30] T. A. L. Burgo, B. C. Batista, F. Galembeck, *ACS Omega* **2017**, *2*, 8940.
[31] Z. Chen, A. Khajeh, A. Martini, S. H. Kim, *Sci. Adv.* **2019**, *5*, eaaw0513.
[32] Electricity on Rubber Surfaces: A New Energy Conversion Effect | ACS Omega, (n.d), https://pubs.acs.org/doi/full/10.1021/acsomega.7b01010 (accessed: September 2020).
[33] J. Xiong, P. Cui, X. Chen, J. Wang, K. Parida, M.-F. Lin, P. S. Lee, *Nat. Commun.* **2018**, *9*, 4280.
[34] W. Zhang, S. H. Brongersma, O. Richard, B. Brijs, R. Palmans, L. Froyen, K. Maex, , *Microelectron. Eng.* **2004**, *76*, 146.
[35] D. Kiesewetter, R. R. Jones, A. Camper, S. B. Schoun, P. Agostini, L. F. DiMauro, *Nat. Phys.* **2018**, *14*, 68.
[36] W. Du, X. Han, L. Lin, M. Chen, X. Li, C. Pan, Z. L. Wang, *Adv. Mater.* **2014**, *4*, 1301592.
[37] Y. Yang, G. Zhu, H. Zhang, J. Chen, X. Zhong, Z.-H. Lin, Y. Su, P. Bai, X. Wen, Z. L. Wang, *ACS Nano.* **2013**, *7*, 9461.